Digital soil erodibility mapping by soilscape trending and kriging

Fabio Arnaldo Pomar Avalos, Marx Leandro Naves Silva, Pedro Velloso Gomes Batista, Lucas Machado Pontes, Marcelo Silva de Oliveira

Angaben zur Veröffentlichung / Publication details:

Pomar Avalos, Fabio Arnaldo, Marx Leandro Naves Silva, Pedro Velloso Gomes Batista, Lucas Machado Pontes, and Marcelo Silva de Oliveira. 2018. "Digital soil erodibility mapping by soilscape trending and kriging." *Land Degradation & Development* 29 (9): 3021–28. https://doi.org/10.1002/ldr.3057.

DIGITAL SOIL ERODIBILITY MAPPING BY SOILSCAPE TRENDING AND KRIGING

Fabio Arnaldo Pomar Avalos[A], Marx Leandro Naves Silva [A] *, Pedro Velloso Gomes Batista[A], Lucas Machado Pontes[A], Marcelo Silva de Oliveira[B]

[A]Universidade Federal de Lavras, Departamento de Ciência do Solo, Lavras, Minas Gerais, Brasil

[B]Universidade Federal de Lavras, Departamento de Estatística, Lavras, Minas Gerais, Brasil.

Corresponding author*:

Marx Leandro Naves Silva

Address:

Campus Universitário, UFLA/DCS, P.O. Box 3037, Lavras, MG

Tel:

+553538291263

Fax:

+553538291251

E-mail:

marx@dcs.ufla.br

Running Title:

SOIL ERODIBILITY MAPPING

This article has been accepted for publication and undergone full peer review but has not been through the copyediting, typesetting, pagination and proofreading process which may lead to differences between this version and the Version of Record. Please cite this article as doi: 10.1002/ldr.3057

Abstract

Spatial representation of soil erodibility (USLE's K factor) is critical for soil conservation and erosion modeling. K factor is directly linked to the soil properties, whose variability is spatially continuous and related to soilscape. The objective of this study was to test a methodology to map the spatial distribution of soil erodibility in a 1 200 ha sub-basin making use of available spatial covariates and field data. The analysis was run for the Posses sub-basin, in southeast Brazil. The topsoil erodibility was calculated at 85 sampled locations. The spatial prediction of soil erodibility value at each map cell was defined using the scorpan approach, combining: selection of soilscape covariates by multiple linear regression analysis, which was used as the trend term in kriging with external drift (KED). The results confirmed that relief data could produce feasible results for digital soil erodibility mapping, especially when combining with geostatistical procedures. A comparison with ordinary kriging, showed better error statistics for KED and decreased values of the variance of the estimates. This could affect significantly the uncertainty of further USLE applications. The best agreement between erodibility KED model and direct measurements of the K factor, available in the literature, was observed for the Red-Yellow Argisol (Red-Yellow Ultisol), which is the dominant soil class in the sub-basin.

Keywords: geostatistics, remote sensing, K factor, USLE

INTRODUCTION

Soil erosion is one of the main causes of land degradation (Lal, 2001; Montgomery, 2007). Hence, the knowledge and description of erosion linked processes are critical in order to promote soil sustainability. Spatial representation of soil erodibility is decisive for allocation of soil conservation practices, site-based land management, and soil erosion modeling (Auerswald *et al.*, 2014; Panagos *et al.*, 2014; Renard *et al.*, 1997). Soil erodibility represents soil susceptibility to suffer detachment by hydric erosion process. In the Universal Soil Loss Equation (USLE), the most widely used erosion prediction model, such parameter is defined as a ratio between soil loss measured in a unit plot and rainfall erosivity (Wischmeier & Smith, 1978). Where these measurements are not available, soil erodibility can be estimated based on soil attributes (Renard *et al.*, 1997; Wischmeier & Smith, 1978). However, soil erodibility mapping and further USLE applications have been commonly applied on discrete soil maps, disregarding the continuous spatial variability of this parameter (e.g. Iaaich *et al.*, 2016; Zolin *et al.*, 2011).

Recently, spatial statistics methods have been applied to take account the continuum lateral variation of soil erodibility or soil attributes that are used for its calculation. For example, Addis and Klick (2015) applied ordinary kriging (OK) on Wischmeier's nomograph values, whereas Pérez-Rodriguez (2007) applied OK on parameters that were used to calculate soil erodibility, i.e. silt, clay and organic matter. Even though these works report a good performance for the OK method, the stationarity assumption that supports its feasibility cannot be guaranteed (McBratney *et al.*, 2006; Oliver & Webster, 2014).

Stationarity dictates a constant mean (no trend) in the data, while soil properties are determined by the soil forming factors. The effects of these factors on the variability (spatial or not) of any soil attribute are scale dependent (Jenny, 1941; McBratney *et al.*, 2006). Consequently, in order to apply a kriging method, trend modeling is required.

The *scorpan* approach is an extension of the Hans Jenny's state equation of soil formation factors (Jenny, 1941). On this, *s* stands for soil, *c* for climate, *o* for organisms and vegetation, *r* for relief, *p* for parent material, *a* for age and *n* for location (McBratney *et al.*, 2003). This approach establishes a method to estimate the empirical relation between a soil attribute and the spatial representation of any available soil forming factor, and also deals with spatially autocorrelated error. Then, a trend model that links the target soil property with one or more available soil forming factor representation (spatial covariate) is estimated and residuals can be interpolated.

Remotely sensed data offer systematic measurements of land surface features for a certain spatial resolution, as in digital elevation models (DEM) or reflectance imagery (Jensen, 2007). Its current availability represents a huge potential in soil mapping applications (Levi & Rasmussen, 2014; Mulder *et al.*, 2011). Hence, trend modeling using terrain attributes (DEM derived) and vegetation indexes (reflectance ratios) as soilscape proxies are suitable to be used as spatial covariates in trend modeling, in this case, for soil erodibility.

The objective of this study was to test a methodology to model the continuous lateral distribution of soil erodibility in a 1 200 ha sub-basin, making use of spatial covariates as soilscape proxies and kriging.

MATERIAL AND METHODS

Study area

This study was carried out in the Posses sub-basin, located in the south of State of Minas Gerais, Brazil. The watershed has an approximate area of 1 200 ha and altitudes between 968 and 1 420 m (ure 1). Relief is very undulated (slopes between 20 to 45 %) to

undulated (8 to 2 %) (Silva et al., 2013). Regional climate, according to Köppen's criteria, is Cfb, i.e. subtropical without dry season (Alvares *et al.*, 2013).

Land use in the watershed is mainly grassland (64%), permanent preservation areas, which are currently being reforested (18%), and Atlantic native forest (13%) (Silva *et al.*, 2013). Soil classes, according to Brazilian Soil Classification System (Embrapa, 2013) and their correspondence with Soil taxonomy (USDA, 2014) are: Red-Yellow Argisol - RYA (Red-Yellow Ultisol), Haplic Cambisol - HaC (Ochrept), Humic Cambisol - HuC (Inceptisol), Fluvic Neosol - FN (Fluvent) and Litholic Neosol - LN (Udorthent) (Figure 1).

Field data and point erodibility calculation

Soil erodibility calculation involved 85 point samples from the 0 - 0.2 m soil layer. Point sampling distribution was intended to be at a regular spacing; however, due to the low accessibility condition of the area, it was not possible to visit some points and opportunistic sampling locations were collected. Nevertheless, point-pattern distribution of the current dataset presents an average nearest neighbor distance of 247.4 m and corresponds with a dispersed pattern (expected random distance = 188.6 m, $Z = 5.50$, $P < 0.01$). The proportion of point samples maintains a good agreement with the occurrence of soil classes in the area (Figure 1), where RYA and HaC are the dominant classes with 40.8 and 29.6 % of the sub-basin area, and point sample proportions of 28.2 and 36.5 %. Less expressive soil classes, i.e. HuC (11.5%), FN (10.3%) and LN (7.7%) registered sample proportions of 8.2, 17.6 and 9.4 %, respectively.

Samples were submitted to laboratory analysis, in accordance with EMBRAPA (1997), in order to determine saturated hydraulic conductivity (mm h^{-1}) and sand, very fine sand, silt, clay and organic matter mass fractions (%). Soil structure classes were assigned to

each point based on measurements from 21 soil profiles and the soil class associated to the particular point location (Silva *et al.*, 2013).

A Wischmeier's nomograph (Wischmeier *et al.*, 1971) approximation established by Auerswald *et al.* (2014) was applied on laboratory data. On this approximation, nomograph divergences caused by very low erodibility values, as well as those caused by high silt (≥70%) and organic high matter (≥4%) content, are minimized. Hence, soil erodibility (K) is calculated as:

$$\mathrm{K}_1 = \begin{cases} 2.77\times10^{-5}\times\left(\varphi_{Si+vfSa}\times\left(100-\varphi_{\mathrm{Cl}}\right)\right)^{1.14}, \varphi_{Si+vfSa} < 70\% \\ 1.75\times10^{-5}\times\left(\varphi_{Si+vfSa}\times\left(100-\varphi_{\mathrm{Cl}}\right)\right)^{1.14} \\ +\,0.0024\times\varphi_{Sa-vfSa}+0.16, \varphi_{Si+vfSa}\geq 70\% \end{cases} \quad \text{(Eq. 1)}$$

$$\mathrm{K}_2 = \begin{cases} \dfrac{12-\varphi_{\mathrm{OM}}}{10}, \varphi_{\mathrm{OM}} < 4\% \\ 0.8, \varphi_{\mathrm{OM}}\geq 4\% \end{cases} \quad \text{(Eq. 2)}$$

$$\mathrm{K} = \begin{cases} \mathrm{K}_1\times\mathrm{K}_2+0.043\times\left(\mathrm{A}-2\right)+0.033\times\left(\mathrm{P}-3\right), \mathrm{K}_1\times\mathrm{K}_2 > 0.2 \\ 0.091-0.34\times\mathrm{K}_1\times\mathrm{K}_2+1.79\times\left(\mathrm{K}_1\times\mathrm{K}_2\right)^2 \\ +\,0.24\times\mathrm{K}_1\times\mathrm{K}_2\times\mathrm{A}+0.033\times\left(\mathrm{P}-3\right), \mathrm{K}_1\times\mathrm{K}_2\leq 0.2 \end{cases} \quad \text{(Eq. 3)}$$

where: K is soil erodibility (t ha^{-1} h N^{-1}), $\varphi_{Si+vfSa}$ is silt and very fine sand (2 – 100 μm) mass fraction (%) , φ_{Cl} is mass fraction (%) of clay (2 < μm) and φ_{OM} is organic matter mass fraction (%) in the fine dried earth (< 2 mm) fraction. A is the soil structure index: very fine granular = 1, fine granular = 2, medium or coarse granular = 3 and blocky, platy or massive = 4; P is soil permeability index: very fast = 1, moderate fast = 2, moderate = 3, moderate slow = 4, slow = 5, very slow = 6. A summary of the registered values in samples is presented in Table 1. Since K is expressed in t ha^{-1} h N^{-1}, we divided these values by 10 in order to use SI conventional units (t ha MJ^{-1} mm^{-1}).

Model analysis

In order to establish a quantitative relationship between soil erodibility and spatial covariates, scorpan approach has been applied (McBratney *et al.*, 2006). In this case, the evaluation of a drift function enables the modeling of a soil property as a response of spatial representations (spatial covariates) of soil formation factors. Moreover, spatially autocorrelated error (drift function residuals) is also explicitly defined.

Scorpan's *r* and *o* factors, i.e. relief and organisms - vegetation representations, are the most widely applied in soil mapping applications. This is due to the availability of digital elevation models (DEM) and the outstanding number of terrain attributes that are derived from them. The same can be said about surface reflectance imagery and derived indexes, like the normalized difference vegetation index (NDVI).

Climate and parent material covariates are not available at the scale used in the model. Current maps show null to very low spatial variability, in contrast to relief and organisms and vegetation factors.

An SRTM image with a spatial resolution of 30 m was employed as DEM of the study area. The software SAGA, version 2.1.4 (Conrad *et al.*, 2015), was used to correct spurious depressions in surface data and for the generation of the following terrain attributes: convergence index (CI), channel network base level (CNBL), cross-sectional curvature (CSC), longitudinal curvature (LC), contribution area (LOGCA), relative slope position (RSP), slope (SLP), valley depth (VD), vertical distance to channel network (VDCN) and topographic wetness index (TWI). Besides elevation (ELEV), this set of covariates was assumed as the relief factor (*r*) in scorpan.

Organisms and vegetation and factor, *o* in scorpan model, was represented by a NDVI image and red and near-infrared reflectance data, which were derived on top of the

atmosphere reflectance data from Landsat 5 TM imagery (Chander *et al.*, 2009). The analysis was run on standardized values (zero mean and unit variance). Both topographic and reflectance data were downloaded from the earthengine.google.com site.

Multiple linear regression analysis (MLR) involved K values as the dependent variable and the *r* and *o* proxies as (spatial) covariates, with 3 parameters for *o* factor and 11 in the case of *r* factor. Ordinary least squares (OLS) method was used to fit the model. Best subset procedure and Schwarz bayesian information criterion (BIC) were applied to find the most efficient covariates for the model. Every parameter combination per model is tested for this methodology. Then, the model with the lowest BIC value is used to select efficient covariates, which were used to model the deterministic term in KED.

OLS residuals were submitted to variogram analysis, which involved empirical semivariance calculation by the Matheron's method of moments and the assessment and fitting of three authorized models: Spherical, Exponential and Gaussian. Visual analysis and residual sum of squares (RSS) criteria were applied for the selection of the best-fitted model (Oliver & Webster, 2014).

To test the performance of this approach, a comparison with ordinary kriging mapping (analysis of original K values) was evaluated.

Once determined, variogram models of original and detrended data (OLS residuals) were used for OK and KED estimation, respectively. Besides the variogram model, the trend model defined by the spatial covariates selected in regression analysis was taken as determinant parameters in the KED procedure. Geostatistical analysis was carried out using the gstat package in the R environment (Pebesma, 2004; R-Core-Team, 2015).

Accuracy assessment of KED and OK methods was based on mean error (ME), root mean square error (RMSE) and mean squared deviation ratio (MSDR), which were calculated

according to the results from a leave-one-out cross-validation (Bennett *et al.*, 2013; Oliver & Webster, 2015). Variance of OK and KED predictions were also compared, since it is frequently disregarded and, as uncertainty measure, is quite relevant in further USLE applications.

Soil erodibility outputs from the best model were used to produce erodibility distributions for the soil classes in the sub-basin, this were presented in boxplots with experimental values of soil erodibility direct measurements, obtained from the literature, overlaid to them.

RESULTS AND DISCUSSION

Best-fitted soilscape model for deterministic variability involved only relief parameters: CI, LC and SLP, which showed low but significant linear relationship with soil erodibility (R^2 = 0.31, $F_{8,76}$ = 4.14, P < 0,01, BIC = -1.39). Relief covariates were also identified as important map predictors for soil erodibility by Panagos *et al.* (Panagos *et al.*, 2012) and Teng *et al.* (2016). These authors also identified remotely sensed data as important predictors of soil erodibility, which in this study were excluded by the model, since remote observation of soil properties is dependent of the proportion of bare soil cover, and this is insignificant in the Posses sub-basin (ca. 2.7 %) (Lima *et al.*, 2013) preventing the use of reflectance related metrics.

Although the variance proportion explained by the deterministic model (30%) was low, its statistical significance was expected by the regionalized variable model, since variability isn't modeled completely by the deterministic component (Hengl *et al.*, 2007).

Hengl *et al.* (2004) showed that coefficients of determination below 0.5 and bounded spatial structure for residuals are expected to show good performances for the kriging with external drift methods. This is because regression models with very high R^2 values would

explain most part of the variability in the deterministic term, making no use of spatial estimation of residuals.

Estimated parameters for the variograms indicated that best fit model for original K values is Exponential, whereas the detrended data was best fitted according to a Spherical model (Table 2). Such pattern was also expected for non-stationary data, given that after a significant fit for the trend model, variance is reduced and a bounded variogram (Spherical) function represents a reduction in spatial variability in contrast with an asymptotically bounded model (Exponential) (Oliver & Webster, 2014, 2015). Addis *et al*. (2015), also analyzing USLE nomograph values, found that the best model for soil erodibility spatial autocorrelation structure was a Gaussian model, but with a clear unbounded pattern. Such structure could be an indicator of a trend on the analyzed data.

Figure 2 displays the best-fitted variogram models for the OLS residuals and the original data. The reduction of the sill and range parameters of the residual semivariogram in comparison to target variable semivariogram indicates that feature-space structure has decreased, as an effect of the trend removal using deterministic modeling. This behavior shows the influence that a soil forming factor as relief could have on the spatial pattern of soil properties.

Mean error (ME) of cross-validation results for KO and KED were similar and very close to zero. Such values are expected since kriging estimations are unbiased, even with poorly chosen models (Oliver & Webster, 2014). However, improvements were registered on RMSE and MSDR for the KED method (Table 3).

OK and KED maps of soil erodibility and respective estimation variances are presented in Figure 3. Low sampling density has a marked effect in OK estimation uncertainty (high variance patches, Fig 3c), which was diminished in KED method, since the trend model represents 30% of the variability in the data and registered the lowest MSDR

value (Table 3). Such variance reduction effect was calculated at 92% of the sub-basin, notably in areas with poor point sampling.

Nevertheless, higher variance regions, both in OK and KED maps, located in the watershed divide are the result of misrepresentation of feature and geographic spaces by the point sampling. Map accuracy should not be interpreted based on global statistics only, as pointed out by Buttafuoco *et al.* (2012) and Castrignanò *et al.*, (2008). Since maps are modeling outputs, is expected that its uncertainty follows a spatial pattern.

Soil erodibility output values based on the KED model (Figure 3B) ranged from 0.57 to 5.32 (10^2 t h MJ^{-1} mm^{-1}), mean and standard deviation were 2.26 and 0.54 (10^2 t h MJ^{-1} mm^{-1}). Regarding specific soil classes, a comparison with erodibility values from other studies that estimated soil erodibility directly (i.e. using soil loss measurements from unit plots under natural or simulated rainfall) in contrasting regions of Brazil is presented in Figure 4. Among these, best agreement is observed for the RYA class (Red-Yellow Ultisol) (Eduardo *et al.*, 2013; Marques *et al.*, 1997a, 1997b; Sá *et al.*, 2004), which is the dominant soil in the sub-basin (40.8 % of the area) with a KED median value of 2.20 (10^2 t h MJ^{-1} mm^{-1}). In contrast, HaC (Ochrept) (Silva *et al.*, 2009), HuC (Inceptisol) (Bertol *et al.*, 2002) and LN (Udorthent) (Margolis *et al.*, 1985; Silva *et al.*, 1986) show deviance from their correspondent KED median values (HaC = 2.40, HuC = 2.15, LN = 1.94). However, these direct measurement data are within the range produced by the model (Figure 4). No experimental value for the FN class was found in the literature.

According to Figure 4, erodibility values for the LN soil class were overestimated. Such behavior can be partially explained by correction factor for very low K values used in equation 2. Also, the erodibility values determined directly on field plots for such soil class are based on experiments from a semi-arid region of the Brazilian northeast (Margolis *et al.*,

1985; Silva *et al.*, 1986). Hence, some variability of soil properties can be expected in relation to the ones observed in this study, even within the same soil class.

The discrepancies between KED model estimations and K values from direct experiments reported in the literature can be mostly attributed to the formulas used for determining K indirectly. Such discrepancies seem to be more evident in the LN and HaC soil classes ;. Although Wischmeier's nomograph has been widely used for estimating K values, the works from Marques *et al.* (1997a) and Silva *et al.* (2000) indicate that the correlation between K values determined directly and indirectly for Brazilian soils can be very low. Nevertheless, our work shows that once such formulas are optimized, terrain attributes can be used to improve spatial estimations of erodibility values.

Spatial applications of USLE model are supported by the interaction of spatial representations of five factors, namely: rainfall-runoff erosivity, soil erodibility, topography (length and slope), vegetation cover and conservation practices (Renard *et al.*, 1997). Uncertainty in model outputs could be decreased as an effect of the reduction of estimation variance in the soil erodibility parameter (Buttafuoco *et al.*, 2012; Teng *et al.*, 2016), as we showed.

CONCLUSIONS

Soilscape terrain attributes present low but significant linear relation with soil erodibility. Trend modeling of soil erodibility brings reliability for the stationarity assumption in kriging method.

Compared with ordinary kriging, besides better error statistics, estimate variance in kriging with external drift (KED) was minor in the most of the sub-basin area, and this may have implications in uncertainty propagation for further USLE mapping applications.

The soil erodibility values from KED model have the best agreement with the Red-Yellow Argisol soil class. This may serve as a methodology optimization regarding the erodibility mapping of this particular soil class.

Acknowledgements

This research was funded in part by Coordination of Superior Level Staff Improvement – CAPES, the National Counsel of Technological and Scientific Development– CNPq (Process No. 305010/2013-1), and Minas Gerais State Research Foundation – FAPEMIG (Process No. CAG-APQ 01053-15).

References

Addis HK, Klik A. 2015. Predicting the spatial distribution of soil erodibility factor using USLE nomograph in an agricultural watershed, Ethiopia. *International Soil and Water Conservation Research* **3**: 282–290. DOI: 10.1016/j.iswcr.2015.11.002

Alvares CA, Stape JL, Sentelhas PC, de Moraes Gonçalves JL, Sparovek G. 2013. Köppen's climate classification map for Brazil. *Meteorologische Zeitschrift* **22**: 711–728. DOI: 10.1127/0941-2948/2013/0507

Auerswald K, Fiener P, Martin W, Elhaus D. 2014. Use and misuse of the K factor equation in soil erosion modeling: An alternative equation for determining USLE nomograph soil erodibility values. *Catena* **118**: 220–225. DOI: 10.1016/j.catena.2014.01.008

Bennett ND, Croke BFWW, Guariso G, Guillaume JHAA, Hamilton SH, Jakeman AJ, Marsili-Libelli S, Newham LTHH, Norton JP, Perrin C, Pierce SA, Robson B, Seppelt R, Voinov AA, Fath BD, Andreassian V. 2013. Characterising performance of environmental models. *Environmental Modelling and Software* **40**: 1–20. DOI: 10.1016/j.envsoft.2012.09.011

Bertol I, Schick J, Batistela O, Leite D, Amaral A. 2002. Erodibilidade de um Cambissolo Húmico sob chuva natural entre 1989 e 1998 em Lages (SG). *Revista Brasileira de Ciência do Solo* **26**: 465–471

Buttafuoco G, Conforti M, Aucelli PPC, Robustelli G, Scarciglia F. 2012. Assessing spatial uncertainty in mapping soil erodibility factor using geostatistical stochastic simulation. *Environmental Earth Sciences* **66**: 1111–1125. DOI: 10.1007/s12665-011-1317-0

Castrignanò A, Buttafuoco G, Canu A, Zucca C, Madrau S. 2008. Modelling spatial uncertainty of soil erodibility factor using joint stochastic simulation. *Land Degradation & Development* **19**: 198–213. DOI: 10.1002/ldr.836

Chander G, Markham BL, Helder DL. 2009. Summary of current radiometric calibration coefficients for Landsat MSS, TM, ETM+, and EO-1 ALI sensors. *Remote Sensing of Environment* **113**: 893–903. DOI: 10.1016/j.rse.2009.01.007

Conrad O, Bechtel B, Bock M, Dietrich H, Fischer E, Gerlitz L, Wehberg J, Wichmann V, Böhner J. 2015. System for Automated Geoscientific Analyses (SAGA) v. 2.1.4. *Geoscientific Model Develoment* 1991–2007. DOI: 10.5194/gmd-8-1991-2015

Eduardo EN, Carvalho DF, Machado RL, Soares PFC, Almeida WS. 2013. Erodibilidade, fatores cobertura e manejo e práticas conservacionistas em argissolo vermelho-amarelo, sob condições de chuva natural. *Revista Brasileira de Ciencia do Solo* **37**: 796–803. DOI: 10.1590/S0100-068320130003000026

Empresa Brasileira de Pesquisa Agropecuaria - EMBRAPA. 2013. *Sistema Brasileiro de Classificação de Solos*. Brasília

Empresa Brasileira de Pesquisa Agropecuaria - EMBRAPA. 1997. *Manual de métodos de análise de solo*. Ministério da Agricultura: Rio de Janeiro

Hengl T, Heuvelink GBM, Rossiter DG. 2007. About regression-kriging: From equations to case studies. *Computers & Geosciences* **33**: 1301–1315. DOI: 10.1016/j.cageo.2007.05.001

Hengl T, Heuvelink GBM, Stein A. 2004. A generic framework for spatial prediction of soil variables based on regression-kriging. *Geoderma* **120**: 75–93. DOI: 10.1016/j.geoderma.2003.08.018

Iaaich H, Moussadek R, Baghdad B, Mrabet R, Douaik A, Abdelkrim D, Bouabdli A. 2016. Soil erodibility mapping using three approaches in the Tangiers province –Northern Morocco. *International Soil and Water Conservation Research* **4**: 159–167. DOI: 10.1016/j.iswcr.2016.07.001

Jenny H. 1941. *Factors of Soil Formation, A System of Quantitative Pedology*. McGraw-Hill: New York

Jensen JR. 2007. *Remote sensing of the environment: an earth resource perspective*. *Prentice Hall, Upper Saddle River, NJ*. Pearson Prentice Hall

Lal R. 2001. Soil degradation by erosion. *Land Degradation & Development* **12**: 519–539. DOI: 10.1002/ldr.472

Levi MR, Rasmussen C. 2014. Covariate selection with iterative principal component analysis for predicting physical soil properties. *Geoderma* **219**–**220**: 46–57. DOI: 10.1016/j.geoderma.2013.12.013

Lima GC, Silva MLN, Curi N, Silva MA da, Oliveira AH, Avanzi JC, Ummus ME. 2013. Evaluation of vegetation cover using the normalized difference vegetation index (NDVI). *Ambiente e Agua - An Interdisciplinary Journal of Applied Science* **8**: 204–214. DOI: 10.4136/ambi-agua.959

Margolis E, Silva A, Jaques F. 1985. Determinação dos fatores da equação universal das perdas de solo para as condições de Caruaru (PE). *Revista Brasileira de Ciencia do Solo* **9**: 165–169

Marques JJGSM, Curi N, Ferreira MM, Lima JM, Silva MLN, Carolino de Sá MA. 1997a. Adequação de métodos indiretos para estimativa da erodibilidade de solos com horizonte B textural no Brasil. *Revista Brasileira de Ciência do Solo* 447–456

Marques JJGSM, Curi N, Lima JM, Ferreira MM, Silva M, Ferreira D. 1997b. Estimativa da

erodibilidade a partir de atributos de solos com horizonte B textural no Brasil. *Revista Brasileira de Ciencia do Solo* 457–465

McBratney A., Mendonça Santos M., Minasny B. 2003. On digital soil mapping. *Geoderma* **117**: 3–52. DOI: 10.1016/S0016-7061(03)00223-4

McBratney A, Mendoça Santos M, Minasny B. 2006. On digital soil mapping. *Geoderma* **117**: 3–52. DOI: 10.1016/S0016-7061(03)00223-4

Montgomery DR. 2007. Soil erosion and agricultural sustainability. *Proceedings of the National Academy of Sciences of the United States of America* **104**: 13268–72. DOI: 10.1073/pnas.0611508104

Mulder VLL, de Bruin S, Schaepman MEE, Mayr TRR. 2011. The use of remote sensing in soil and terrain mapping — A review. *Geoderma* **162**: 1–19. DOI: 10.1016/j.geoderma.2010.12.018

Oliver MA, Webster R. 2014. A tutorial guide to geostatistics: Computing and modelling variograms and kriging. *Catena* **113**: 56–69. DOI: 10.1016/j.catena.2013.09.006

Oliver MA, Webster R. 2015. *Basic Steps in Geostatistics: The Variogram and Kriging*. Springer International Publishing. DOI: 10.1007/978-3-319-15865-5

Panagos P, Meusburger K, Alewell C, Montanarella L. 2012. Soil erodibility estimation using LUCAS point survey data of Europe. *Environmental Modelling & Software* **30**: 143–145. DOI: 10.1016/j.envsoft.2011.11.002

Panagos P, Meusburger K, Ballabio C, Borrelli P, Alewell C. 2014. Soil erodibility in Europe: a high-resolution dataset based on LUCAS. *The Science of the total environment* **479–480**: 189–200. DOI: 10.1016/j.scitotenv.2014.02.010

Pebesma EJ. 2004. Multivariable geostatistics package in S: the gstat package. *Computers & Geosciences* **30**: 683–691

Pérez-Rodríguez R, Marques MJ, Bienes R. 2007. Spatial variability of the soil erodibility parameters and their relation with the soil map at subgroup level. *Science of The Total Environment* **378**: 166–173. DOI: 10.1016/j.scitotenv.2007.01.044

R-Core-Team. 2015. R: A language and environment for statistical computing. R Foundation for Statistical Computing. Vienna, Austria

Renard K, Foster G, Weesies G, McCool D, Yoder D. 1997. *Predicting Soil Erosion by Water: A Guide to Conservation Planning With the Revised Universal Soil Loss Equation*. U.S. Department of Agriculture: Washington

Sá MAC de, Lima JM de, Curi N, Massaroto JA, Marques JJG de S e M. 2004. Estimativa da erodibilidade pela desagregação por ultra-som e atributos de solos com horizonte B

textural. *Pesquisa Agropecuária Brasileira* **39**: 691–699. DOI: 10.1590/S0100-204X2004000700011

Silva AM, Silva MLN, Curi N, Avanzi JC, Ferreira MM. 2009. Erosividade da chuva e erodibilidade de Cambissolo e Latossolo na região de Lavras, Sul de Minas Gerais. *Revista Brasileira de Ciencia do Solo* **33**: 1811–1820. DOI: 10.1590/S0100-06832009000600029

Silva IF, Andrade AP, Campos Filho OR. 1986. Erodibilidade de seis solos do semi-árido paraibano obtida com chuva simulada e método nomográfico. *Revista Brasileira de Ciência do Solo* **10**: 283–287

Silva MA, Freitas DAF, Silva MLN, Oliveira AH, Lima GC, Curi N. 2013. Sistema de informações geográficas no planejamento de uso do solo. *Revista Brasileira de Ciências Agrárias* **8**: 316–323. DOI: 10.5039/agraria.v8i2a2289

Silva M, Curi N, de Lima J, Ferreira M. 2000. Avaliação de métodos indiretos de determinação da erodibilidade de latossolos brasileiros. *Pesquisa Agropecuária Brasileira* 1207–1220

Teng H, Viscarra Rossel RA, Shi Z, Behrens T, Chappell A, Bui E. 2016. Assimilating satellite imagery and visible–near infrared spectroscopy to model and map soil loss by water erosion in Australia. *Environmental Modelling & Software* **77**: 156–167. DOI: 10.1016/j.envsoft.2015.11.024

United States Department of Agriculture - USDA. 2014. *Keys to soil taxonomy*. USDA-NRCS: Washington, DC

Wischmeier W, Johnson C, Cross B. 1971. A soil erodibility nomograph for farmland and construction sites. *Journal of Soil and Water Conservation* **26**: 189–193

Wischmeier WH, Smith DD. 1978. *Predicting rainfall erosion losses. A guide to conservation planning. Predicting rainfall erosion losses-A guide to conservation planning*. USDA, Science and Education Administration: Washington

Zolin CA, Folegatti MV, Mingoti R, Sánchez-Román RM, Paulino J, Gonzáles AMGO. 2011. Minimização da erosão em função do tamanho e localização das áreas de floresta no contexto do programa "conservador das águas." *Revista Brasileira de Ciencia do Solo* **35**: 2157–2166. DOI: 10.1590/S0100-06832011000600030

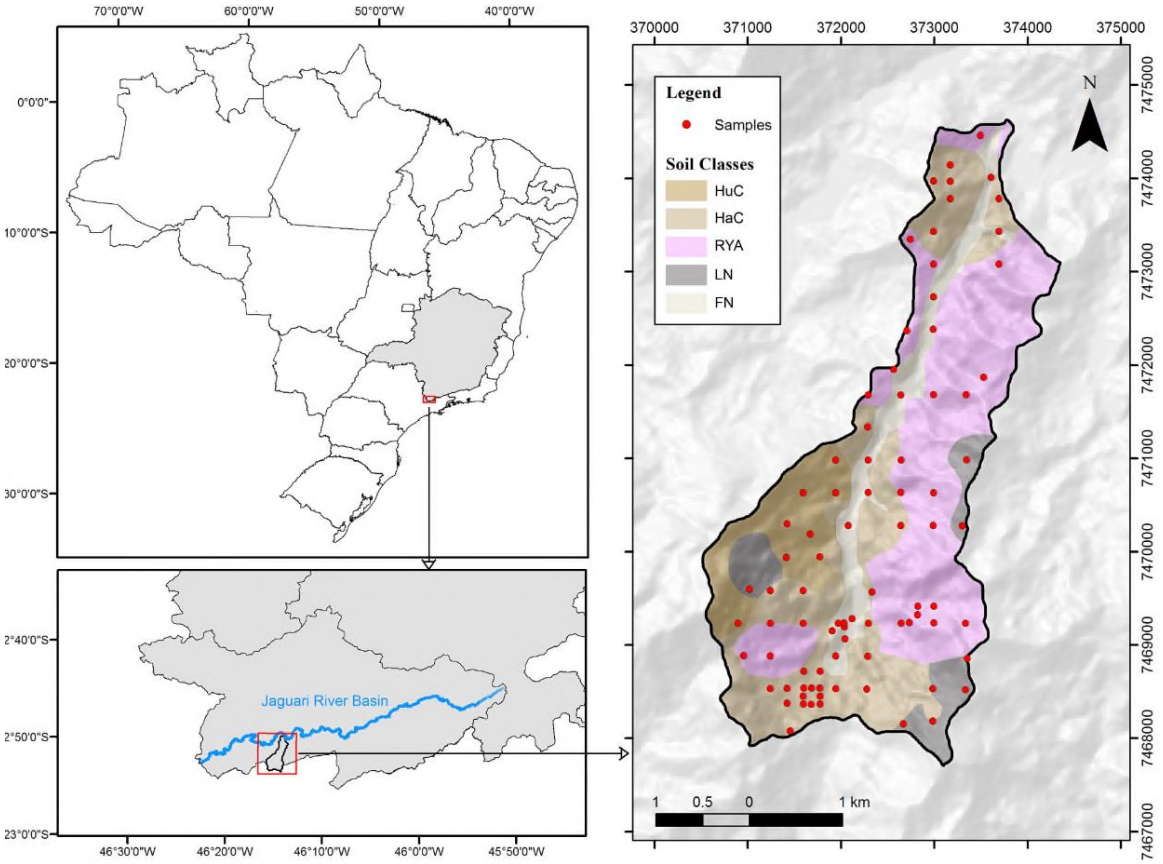

Figure 1. Watershed location, soil classes and spatial distribution of soil samples. Red-Yellow Argisol - RYA (Red-Yellow Ultisol), Haplic Cambisol - HaC (Ochrept), Humic Cambisol - HuC (Inceptisol), Fluvic Neosol - FN (Fluvent) and Litholic Neosol - LN (Udorthent). Coordinate system: Datum SIRGAS 2000, UTM 23K.

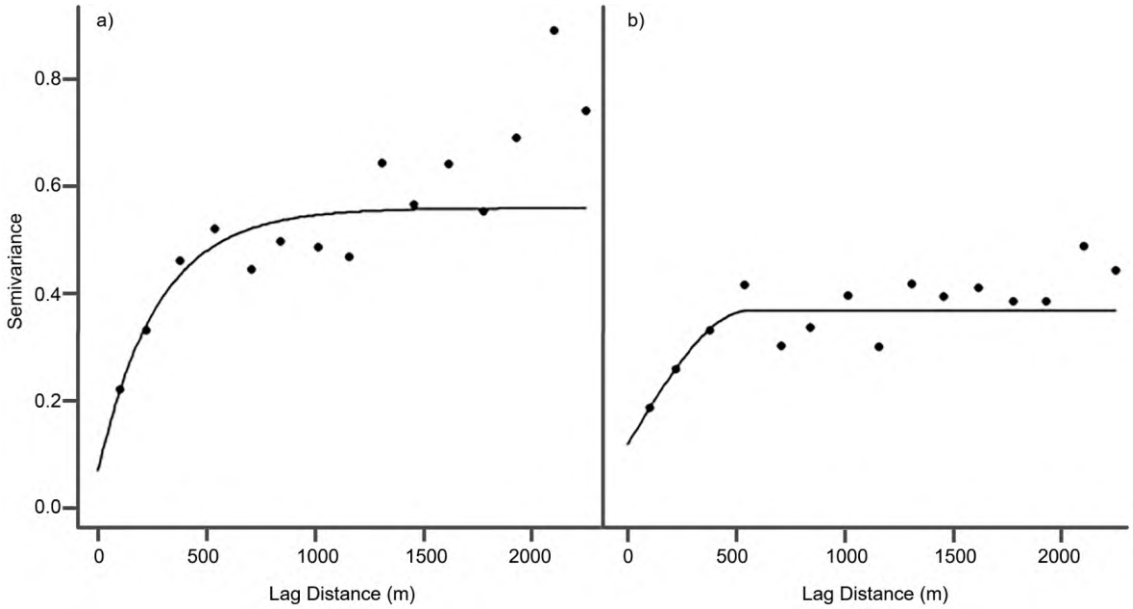

Figure 2. Experimental variograms (dots) and fitted models (lines): original K values and Exponential model (a), detrended data and Spherical model (b).

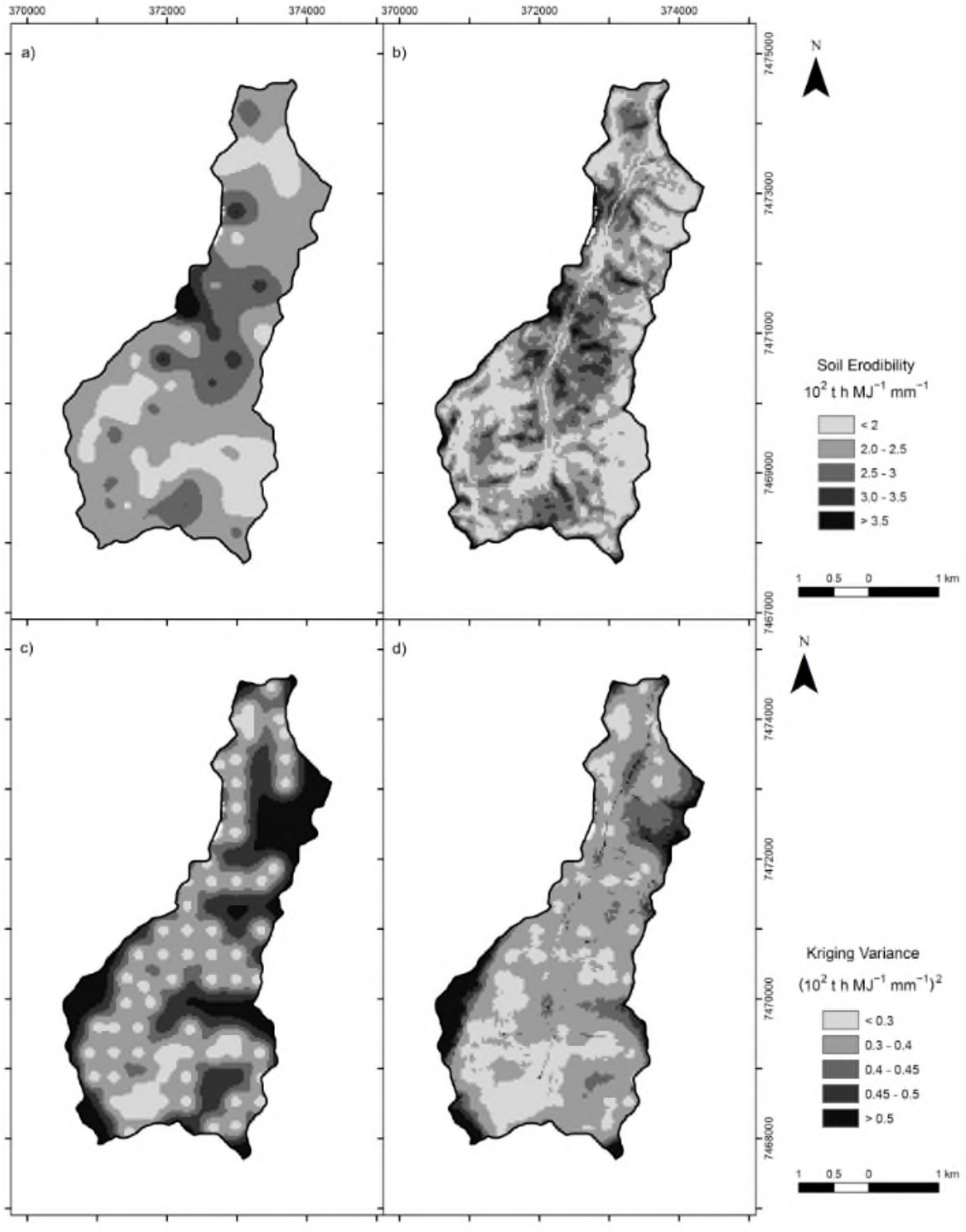

Figure 3. Soil erodibility predictions by OK (a) and KED (b). Variance of OK (c) and KED (d) predictions. Coordinate system: Datum SIRGAS 2000, UTM 23K.

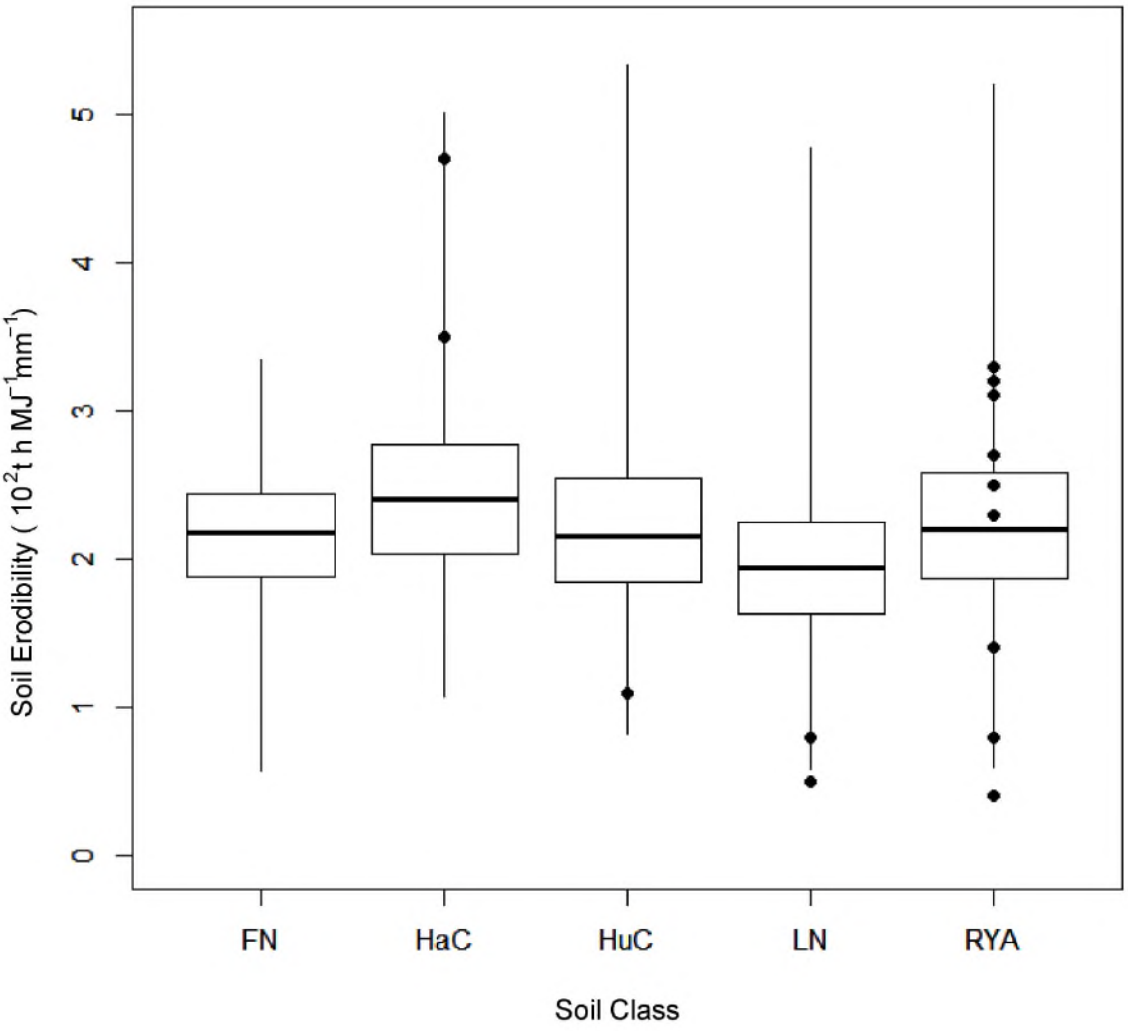

Figure 4. Comparison of soil erodibility by soil class based on KED model outputs (boxplots) and experimental data (dots) obtained in the literature. Red-Yellow Argisol - RYA (Red-Yellow Ultisol), Haplic Cambisol - HaC (Ochrept), Humic Cambisol - HuC (Inceptisol), Fluvic Neosol - FN (Fluvent) and Litholic Neosol - LN (Udorthent).

Table 1.

Soil attributes used in soil erodibility calculation

Attribute	Range	Average	Std. Dev.	CV %
Organic matter (g kg^{-1})	4.0 – 85.0	36.9	14.1	38.3
Saturated hydraulic conductivity (mm h^{-1})	0.0– 85.0	69.5	16.1	234.7
Clay (g kg^{-1})	28.6 – 548.8	335.8	106.8	31.8
Silt (g kg^{-1})	19.2 – 429.4	235	70.8	30.1
Very fine sand (g kg^{-1})	11.3 – 287.2	48.4	35.4	73.2
Erodibility (t h MJ^{-1} mm^{-1})	0.006 – 0.05	0.02	0.07	33.2

CV: coefficient of variation.

Table 2.

Parameters of models fitted to experimental variograms of erodibility original data (OK) a detrended data (KED)

Kriging method and model	Model parameters					Diagnostics	
	C_0	C_1	C	a	r	RSS	VE
OK							
Spherical	0.11	0.41	0.52	579.01		1.15E-05	0.78
Exponential	**0.07**	**0.49**	**0.56**		**273.57**	**1.10E-05**	**0.88**
Gaussian	0.16	0.36	0.53		236.75	1.56E-05	0.69
KED							
Spherical	**0.12**	**0.25**	**0.37**	**554.56**		**4.45E-06**	**0.68**
Exponential	0.07	0.31	0.38		211.68	5.11E-06	0.82
Gaussian	0.18	0.19	0.37		320.45	5.40E-06	0.51

C0: nugget, C1: partial sill, C: sill, a: range, r: distance parameter (a = 3r, Exponential), (a=sqrt(3)r, Gaussian) RSS: residual sum of squares, VE: variance explained. Chosen models in bold.

Table 3.
Cross-validation statistics for the ordinary kriging (OK) and kriging with external drift (KED) methods

	ME	RMSE	MSDR
OK	-0.002	0.776	1.411
KED	-0.001	0.687	1.317

ME: mean error, RMSE: root mean squared error, MSDR: mean squared deviation ratio.